

RESEARCH

Open Access



# The Gai protein subclass selectivity to the dopamine D<sub>2</sub> receptor is also decided by their location at the cell membrane

Agnieszka Polit\* , Beata Rysiewicz, Paweł Mystek, Ewa Błasiak and Marta Dziedzicka-Wasylewska

## Abstract

**Background:** G protein-coupled receptor (GPCR) signaling via heterotrimeric G proteins plays an important role in the cellular regulation of responses to external stimuli. Despite intensive structural research, the mechanism underlying the receptor–G protein coupling of closely related subtypes of Gai remains unclear. In addition to the structural changes of interacting proteins, the interactions between lipids and proteins seem to be crucial in GPCR-dependent cell signaling due to their functional organization in specific membrane domains. In previous works, we found that Gas and Gai<sub>3</sub> subunits prefer distinct types of membrane-anchored lipid domains that also modulate the G protein trimer localization. In the present study, we investigated the functional selectivity of dopamine D<sub>2</sub> long receptor isoform (D<sub>2</sub>R) toward the Gai<sub>1</sub>, Gai<sub>2</sub>, and Gai<sub>3</sub> subunits, and analyzed whether the organization of Gai heterotrimers at the plasma membrane affects the signal transduction.

**Methods:** We characterized the lateral diffusion and the receptor–G protein spatial distribution in living cells using two assays: fluorescence recovery after photobleaching microscopy and fluorescence resonance energy transfer detected by fluorescence-lifetime imaging microscopy. Depending on distribution of data differences between Ga subunits were investigated using parametric approach—unpaired *T*-test or nonparametric—Mann–Whitney *U* test.

**Results:** Despite the similarities between the examined subunits, the experiments conducted in the study revealed a significantly faster lateral diffusion of the Gai<sub>2</sub> subunit and the singular distribution of the Gai<sub>1</sub> subunit in the plasma membrane. The cell membrane partitioning of distinct Gai heterotrimers with dopamine receptor correlated very well with the efficiency of D<sub>2</sub>R-mediated inhibition the formation of cAMP.

**Conclusions:** This study showed that even closely related subunits of Gai differ in their membrane-trafficking properties that impact on their signaling. The interactions between lipids and proteins seem to be crucial in GPCR-dependent cell signaling due to their functional organization in specific membrane domains, and should therefore be taken into account as one of the selectivity determinants of G protein coupling.

**Keywords:** Heterotrimeric G proteins, Dopamine D<sub>2</sub> receptor, Functional selectivity, Protein–membrane interaction, FLIM–FRET, FRAP

## Background

Dopamine D<sub>2</sub> receptor (D<sub>2</sub>R) is one of the class A G-protein-coupled receptors (GPCRs), whose interaction with the heterotrimeric GTP-binding proteins (or G proteins) induces various cellular responses. GPCR proteins are the most recognized target by about 35% of the available drugs [1]. For example, the classical drugs used in the

\*Correspondence: a.polit@uj.edu.pl

Department of Physical Biochemistry, Faculty of Biochemistry  
Biophysics and Biotechnology, Jagiellonian University, Gronostajowa 7,  
30-387 Kraków, Poland



© The Author(s) 2020. **Open Access** This article is licensed under a Creative Commons Attribution 4.0 International License, which permits use, sharing, adaptation, distribution and reproduction in any medium or format, as long as you give appropriate credit to the original author(s) and the source, provide a link to the Creative Commons licence, and indicate if changes were made. The images or other third party material in this article are included in the article's Creative Commons licence, unless indicated otherwise in a credit line to the material. If material is not included in the article's Creative Commons licence and your intended use is not permitted by statutory regulation or exceeds the permitted use, you will need to obtain permission directly from the copyright holder. To view a copy of this licence, visit <http://creativecommons.org/licenses/by/4.0/>. The Creative Commons Public Domain Dedication waiver (<http://creativecommons.org/publicdomain/zero/1.0/>) applies to the data made available in this article, unless otherwise stated in a credit line to the data.

treatment of schizophrenia or Parkinson's disease represent the ligands of dopamine receptors. Based on the cellular response induced by their activation, dopamine receptors are divided into two groups: D1-like ( $D_1$ ,  $D_5$ ) and D2-like ( $D_2$ ,  $D_3$ ,  $D_4$ ). The  $D_2R$  long isoform, which is studied in the present work, is a member of the D2-like group. The characteristic feature of this group is the inhibition of adenylyl cyclase, which leads to a decrease in the level of cAMP via interaction with the  $G_{ai/o}$  class of G proteins. By contrast, the D1-like group induces the opposite effect on the level of cAMP by interacting with the  $G_{as}$  subunits, which in turn activates adenylyl cyclase [2, 3].

Depending on the activity of the  $G_{\alpha}$  subunit, the most recognized partners of GPCRs—heterotrimeric G proteins—are divided into four classes as follows:  $G_{i/o}$ ,  $G_s$ ,  $G_q$ , and  $G_{12/13}$ . The heterotrimeric G proteins consist of three components— $\alpha$ ,  $\beta$ , and  $\gamma$ —forming a trimer in an inactive state, which binds the GDP nucleotide. After activation by a receptor, the bound GDP nucleotide is exchanged for GTP, triggering the dissociation of the trimer into a  $G_{\alpha}$  subunit and a  $G_{\beta\gamma}$  dimer; both these components induce various downstream effects leading to many cellular responses. The  $G_{\alpha}$  subunit is composed of two domains: a GTPase domain, which is responsible for autoregulation via GTP hydrolysis; and a helical domain, which interacts with partners such as the RGS proteins (regulator of G protein signaling), effectors, and the  $G_{\beta\gamma}$  dimer. Changes in the conformation of the helical domain are also implicated in the enzymatic cycle and the overall activity of the G proteins [4]. It has been identified that N-terminus is the site of lipidation which enables docking at the surface of the lipid bilayer, while  $G_{\gamma}$  prenylation influences the plasma membrane localization of the G proteins. Furthermore, lipid modifications of the  $G_{\alpha}$  subunit differ among various classes of G proteins. In the case of  $G_{ai}$ , N-myristylation and S-palmitoylation occur, whereas in  $G_{as}$  N- and S-palmitoylation take place. N-acylation of the lipid moiety is irreversible, but it may be insufficient to allow stable docking at the surface of the lipid bilayer [5]. The second reversible modification occurring at the cysteine residue is proposed as one of the mechanisms that regulate the localization and performance of the G proteins. It has been postulated that activation triggered deprivation of cysteine modification can lead to depletion or enrichment of the protein population at different stages of signal transduction [6–10].

$G_{i/o}$  class consists of two subclasses:  $G_{ai}$  and  $G_{ao}$ . The  $G_{ai}$  subclass is composed of  $G_{ai_1}$ ,  $G_{ai_2}$ , and  $G_{ai_3}$  (genes  $GNAI1$ ,  $GNAI2$ ,  $GNAI3$ ), and the  $G_{ao}$  subclass is composed of  $G_{ao_1}$  and  $G_{ao_2}$  (genes  $GNAO1$ ,  $GNAO2$ ). These proteins show profound homology (approximately 70% amino acid sequence identity) but vary in

other features such as electrostatic properties [11]. While  $D_2R$  is expressed mostly in the basal ganglia (as well as in other brain regions such as the midbrain, thalamus, hypothalamus, and cerebral cortex), none of the three  $G_{ai}$  subunits show any regional specificity in the brain and are present in the regions where  $D_2R$  is expressed. However, the mRNA levels of these subunits vary— $G_{ai_2}$  has a similar prevalence as  $G_{ao_1}$ —whereas the levels of  $G_{ai_1}$  and  $G_{ai_3}$  are relatively lower [12].

The following three regions of the  $G_{\alpha}$  subunit are identified to be involved in the interaction with receptor: C-terminal helix,  $\alpha 4$ – $\beta 6$  loop, and to a lesser extent,  $\alpha N$ – $\beta 1$  loop [13, 14]. The last six amino acids in the C-terminus appear to have the most profound impact as a determinant of selectivity in the G protein–receptor interaction [15, 16]. However, the role of the C-terminus of  $G_{\alpha}$  in interactions with receptors is heterogeneous among GPCRs. In particular, in the case of receptors interacting with  $G_{ai}$ , the other regions of this subunit are thought to reduce the impact of its C-terminus in the interaction with the receptor (the  $G_{ai}$  subunits show high similarity in the C-terminal residues, and only  $G_{ai_3}$  differs in the identity of amino acids in two positions). Furthermore, in contrast to other GPCRs, the  $G_{ai}$ -interacting receptors exhibit selectivity toward specific  $G_{\alpha}$  subunits to a greater extent [17]. On the other hand, the second and third intracellular loops (2ICL, 3ICL), together with the transmembrane helix (TM)—TM3, TM5, and TM6, are recognized as the most relevant regions of GPCRs in terms of their interaction with suitable G proteins [18]. Even closely related receptors show differences in the secondary structure of these regions. Changes in the secondary structure of 2ICL and the length of 3ICL are proposed to influence the selectivity toward G proteins [19]. Nevertheless, in the case of both G proteins and GPCRs, these determinants are not fully recognized yet. In addition to the C-terminus of  $G_{\alpha}$  subunit which acts as a determinant of selectivity of receptor–G protein coupling, there exist other determinants (although not so well documented) that are equally, and sometimes even more important in the recognition of G protein by many receptors [16, 17, 20, 21]. The following factors may affect this process: ligand used to stimulate the receptor, time of stimulation, interacting partners (such as RGS, AGS (receptor-independent activators of G protein signaling), and others), receptors oligomerization, and the lipid composition of the cell membrane [15, 22–24].

Dopamine  $D_2R$  is capable of coupling more than one G protein while modulating the formation of cyclic AMP. The ability to inhibit the activity of adenylyl cyclase depends on the ability to couple one, or more, of the  $G_{i/o}$  subunits [25–27]. However, the mechanism by which the

receptor can selectively discriminate between the closely related subtypes of G proteins and involvement of other factors still remains unclear. It has been shown earlier that dopamine D<sub>2</sub>R may differentially couple the G $\alpha$ i and G $\alpha$ o subtypes in a receptor agonist-dependent manner, leading to diverse functional outcomes [25, 27]. However, most of these interactions were analyzed using a system that measures intracellular events (e.g. cAMP accumulation, calcium mobilization) or in isolated membrane fractions (e.g. radioligand binding studies). Since the G $\alpha$ i and G $\alpha$ o proteins are closely related, it is further difficult to separate their signaling when working on isolated membrane fractions. Most of the studies exploring the role of protein–protein interactions neglect the interactions of the signaling proteins with lipids, as well as the participation of the lipid bilayer itself in the processes of signal transduction. One of the important aspects that have not been fully explored is the impact of the plasma membrane on the efficiency and selectivity of the G proteins signaling. The mutual influence of lipids and membrane proteins along with cytoskeleton is considered as a factor that may promote their nanoclustering and organization into dynamic signaling platforms [28, 29].

Similarly, in the case of trimeric G proteins, partitioning occurs in different regions of the cell membrane. A review of the published data indicated that the G $\alpha$ i proteins reside in the ordered parts of the membrane that are rich in cholesterol and sphingolipids [30, 31]. It is assumed that the partitioning process is driven not only by the lipid moieties attached to proteins but also by interaction with other components residing in such clusters (i.e. caveolins) [31, 32]. Moreover, the specific membrane targeting of G proteins is affected by the G $\beta$  $\gamma$  dimer which seems to determine the preference toward the less-ordered segments of the lipid bilayer [31, 33, 34]. These observations indicate that localization may change in different states of the signal transduction process when the G protein trimer dissociates or associates. In addition, it has been postulated that ligand binding induces changes in the localization of GPCRs [35, 36]. Regardless of the signals within proteins, such as palmitoylation which is a signal stated to localize in the ordered membrane regions [37], other factors may also influence the overall outcome in the compartmentalization process.

In the present study, we analyzed the behavior of the three closely related G $\alpha$ i proteins and dopamine D<sub>2</sub>R in a lipid bilayer environment in the context of activation selectivity. We monitored the dynamics and the mutual proximity of D<sub>2</sub>R and G $\alpha$ i<sub>1</sub>, G $\alpha$ i<sub>2</sub>, or G $\alpha$ i<sub>3</sub>, as well as their heterotrimers formed with the G $\beta$ <sub>1</sub> $\gamma$ <sub>2</sub> dimer, using two highly selective and sensitive assays: fluorescence resonance energy transfer (FRET) and fluorescence recovery after photobleaching (FRAP). These approaches allowed

comparing the receptor and G proteins directly at the living cell membrane in their native dynamic environment, without relying on downstream signals such as the production of second messengers. Surprisingly, although the G $\alpha$ i proteins showed high similarity, our results revealed significant differences not only in their rate of lateral diffusion within the plasma membrane but also in their colocalization with dopamine D<sub>2</sub>R. We found that the cell membrane partitioning of particular G $\alpha$ i heterotrimers and dopamine D<sub>2</sub>R showed a good correlation with the efficiency of D<sub>2</sub>R-mediated inhibition of cAMP. These results suggest that the membrane distribution of signaling partners can be investigated in depth in terms of how it contributes to the selectivity of the G protein–receptor coupling. To the best of our knowledge, this is the first report to show that the G $\alpha$ i subunits differ in their membrane-trafficking properties that impact on their signaling, as the membrane localization of the G $\alpha$ i<sub>1</sub>, G $\alpha$ i<sub>2</sub>, and G $\alpha$ i<sub>3</sub> subunits has been considered to be identical so far.

## Methods

### Site-directed mutagenesis

All the genes encoding human G $\alpha$  subunits (GNAI1, GNAI2, GNAI3, GNAS) and dopamine D<sub>2</sub>R long isoform (DRD2L) were purchased from UMR cDNA Resource Center (Bloomsburg, PA, USA), and the sequences of fluorescent proteins (FP) were obtained from Clontech (Mountain View, CA, USA).

The sequences coding for mCitrine or mGFP were inserted into the  $\alpha$ b– $\alpha$ c loop of the human G $\alpha$ i subunits through Overlap Extension PCR Cloning [38]. In the case of G $\alpha$ i<sub>1</sub> and G $\alpha$ i<sub>2</sub>, the sequences were inserted after Ala121, while for G $\alpha$ i<sub>3</sub>, they were inserted after Ala114 [39]. The sequence of FP was flanked by Ser–Gly and Gly–Ser linkers. The mCitrine and mGFP sequences were obtained as described previously [40]. In the G $\alpha$ s subunit, the FP sequence was incorporated between the helical and GTPase domains as described previously [40]. The sequences of all the G $\alpha$  subunit fusion proteins were obtained in a pcDNA3.1+ vector (Invitrogen, Thermo Fisher Scientific, Inc., Waltham, MA, USA). The D<sub>2</sub>R-mCherry construct (with mCherry fused to the C-terminus of D<sub>2</sub>R) was prepared by introducing restriction sites to DRD2 through polymerase chain reaction and then by cloning the dopamine receptor gene into the pmCherry-N1 vector (Clontech) using NheI and XhoI enzymes. Additionally, to ensure the correct location of the described fusion protein in the membrane, it was necessary to extend the linker between the proteins, which was achieved using a 35-amino acid linker with a flexible character consisting of repeated GGSG sequences.

### Cell culture and transfection

The human embryonic kidney 293 cells (HEK293) (ATCC, Manassas, VA, USA) were cultured in Minimum Essential Medium (MEM) (Thermo Fisher Scientific, Inc., Waltham, MA, USA) with 10% fetal bovine serum (FBS) (Sigma Aldrich, Poznań, Poland) under 5% CO<sub>2</sub> at 37 °C. For imaging experiments, the cells were seeded onto sterile glass coverslips and cultured in 30-mm plates, while for determining the levels of cAMP, the cells were seeded onto six-well plates coated with 0.5% gelatin (Type A; BioShop Canada Inc., Montréal, Canada). Transient transfection was performed using the TRANSIT-X2<sup>®</sup> Dynamic Delivery System (Mirus Bio, Madison, WI, USA) according to the manufacturer's instruction. The amounts of DNA used for each experiment were as follows: determination of cAMP levels—0.9 or 1.7 µg DNA per well; FLIM-FRET and FRAP—0.1–0.45 µg DNA per dish. The ratio of DNA (Gα-D<sub>2</sub>R) used was as follows: determination of cAMP levels: 1–1.25; FLIM-FRET and FRAP: 1:1.5; in case of overexpression of trimer, Gβ, Gγ and Gα were used in equimolar DNA amounts. All the experiments were performed 2 or 3 days after transfection.

### Live-cell imaging microscopy

Leica SP5 II SMD confocal microscope (Leica Microsystems, Mannheim, Germany) or Leica TCS SP5 confocal scanning microscope (Leica Microsystems, Mannheim, Germany) with a 63 × 1.4 numerical aperture and a oil-corrected objective lens was used for the observation of cells. Fluorescence of mCitrine or mGFP was acquired at 495–570 nm with an excitation wavelength of 488 nm (argon ion laser), and that of mCherry at 610–700 nm with an excitation wavelength of 594 nm (laser diode). During observation, the cells were kept at 37 °C in an air-steam cube incubator in Dulbecco's Modified Eagle Medium (DMEM-F12; without phenol red) (Thermo Fisher Scientific, Inc., Waltham, MA, USA) supplemented with 2% FBS.

### cAMP level measurements

The concentration of cAMP was determined in cell lysates using cAMP ELISA chemiluminescence kit (STA-500; Cell Biolabs Inc., San Diego, CA, USA). Three days after transfection, the HEK293 cells were stimulated with 1 µM rotigotine hydrochloride (Sigma Aldrich, Poznań, Poland), a D<sub>2</sub>R agonist, for 10 min. Prior to stimulation, the cells transfected with Gαi were incubated in a medium containing 1 µM forskolin (Sigma Aldrich, Poznań, Poland) for 5 min. These prestimulation and stimulation procedures were conducted in MEM supplemented with 0.5% FBS. After stimulation, the cells were harvested and their cAMP concentration was determined

according to the manufacturer's instructions. In each case, four independent experiments were performed in duplicates. Nontransfected cells were used as controls, and the concentrations of cAMP in transfected cells were normalized in comparison with the values determined in controls in each experiment.

### FLIM-FRET measurements

The cells were observed using Leica SP5 II SMD confocal microscope with an integrated module PicoHarp 300 Time-Correlated Single Photon Counting (TCSPC) system (PicoQuant, Berlin, Germany). The experiments were conducted as described earlier in detail [34]. Confocal images of the cells were collected prior to each FLIM measurement. mCitrine (energy donor) and mCherry (energy acceptor) were used as the FRET pair. The FLIM-FRET experiments were carried out on live HEK293 cells expressing appropriate levels of Gα-mCitrine (donor alone: Gα-mCitrine or Gα-mCitrine with Gβ<sub>1</sub>γ<sub>2</sub>) and D<sub>2</sub>R-mCherry (donor and acceptor: Gα-mCitrine with or without Gβ<sub>1</sub>γ<sub>2</sub> and D<sub>2</sub>R-mCherry). Excitation was performed using a pulsed laser diode (Leica; 40 MHz) at 470 nm. Emission from 500 to 550 nm was collected with an avalanche photodiode using a fluorescence band-pass filter. All the images were recorded in 512 × 512 format with an acquisition time of approximately 3–4 min. In each experiment, the cells with only donor and those with donor-acceptor were observed, and the level of fluorescence of mCitrine and mCherry was estimated. In the case of cells treated with rotigotine (1 µM) for the stimulation of D<sub>2</sub>R, the ligand was added immediately after the imaging was started and the images were collected for up to 15 min after stimulation.

To quantify the apparent fluorescence lifetimes in the plasma membrane, we manually selected the regions of cell areas in each image and fitted the fluorescence lifetime histograms with double-exponential decay functions using SymPhoTime software (PicoQuant, Berlin, Germany). In the case of each image, the FRET efficiency was calculated for the FRETing state with the equation:  $E = 1 - (\tau_{DA}/\tau_D)$  by comparing the donor lifetimes in the presence ( $\tau_{DA}$ ) and absence ( $\tau_D$ ) of the acceptor [41].

### FRAP measurements

All the FRAP experiments were performed and results were analyzed as described earlier [40]. As high photostability was required, mGFP-tagged fusion proteins of Gα subunits were used in these experiments. Briefly, the transiently transfected live HEK293 cells were incubated at 37 °C. Just before imaging, the culture medium was replaced with fresh DMEM-F12 medium enriched with 2% FBS. The FRAP images were collected for at least 100 s after the photobleaching impulse using Leica TCS

SP5 confocal scanning microscope equipped with LAS AF software and a  $63 \times 1.4$  NA oil-immersion lens.

### Statistical analysis

Data distribution was determined using Shapiro–Wilk  $W$  test and skewness and kurtosis analysis. Depending on the approach applied (unpaired  $T$ -test for parametric data and Mann–Whitney  $U$  test for nonparametric data), the results are presented as mean  $\pm$  standard error of the mean (SEM) or median  $\pm$  median absolute deviation (MAD). The details of the statistical analysis were described previously [34].

## Results

### Functionality of created fusion proteins

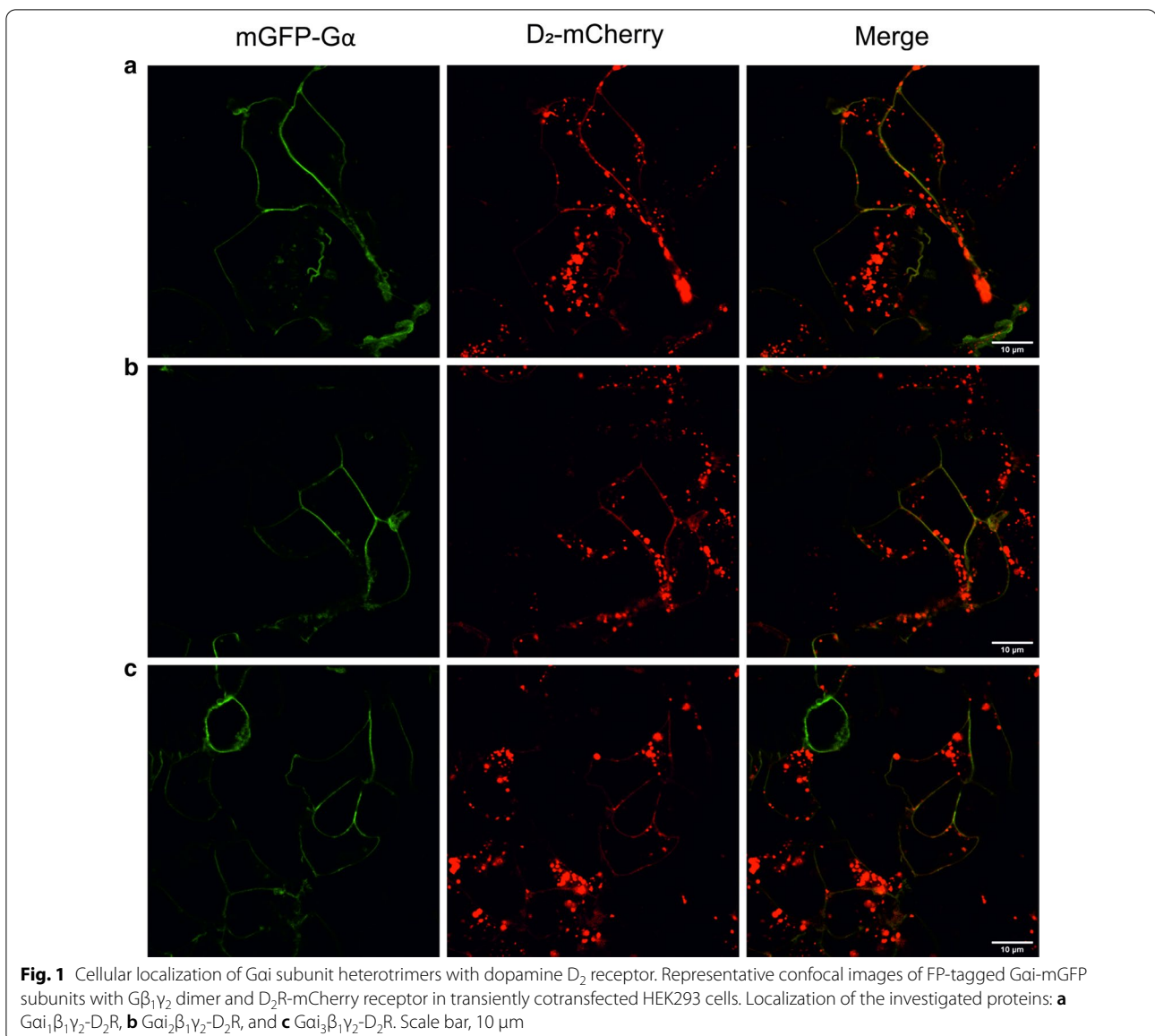
The purpose of this work was to investigate the differences in the coupling selectivity of the three  $G\alpha_i$  subunits of G proteins ( $G\alpha_1$ ,  $G\alpha_2$ ,  $G\alpha_3$ ) toward dopamine  $D_2R$  in living cells. Their mutual colocalization was observed in basal conditions without receptor stimulation and after stimulation with a full agonist—rotigotine. Two approaches were used for analyzing the proteins of interest: FLIM–FRET and FRAP measurements with the use of FPs (mCitrine, mGFP, or mCherry) as tags. Such approaches require more attention during the creation of fusion proteins. In addition, the incorporation of FPs may have a profound impact on the conformation of the investigated proteins and may also influence their functionality, localization and at the tail end—expression level. To address this last uncertainty, we examined the levels of mRNA of all  $G\alpha$ -FP fusion proteins used in co-expression with dopamine  $D_2$  receptor with or without company of  $G\beta\gamma$  subunits. We saw, that the relative expression of studied proteins remained constant in each experimental set-up (Additional file 1).

In the case of  $G\alpha_i$  proteins, mCitrine or mGFP was incorporated into the second loop ( $\alpha\beta$ – $\alpha\gamma$ ) after A114 ( $G\alpha_3$ ) or A121 ( $G\alpha_1$ ,  $G\alpha_2$ ), flanked with short linkers, based on the results reported by Gibson and Gilman for  $G\alpha_3$  [34, 39]. This process minimizes the possibility of disruption of the interaction between the  $G\alpha$  subunit and  $D_2R$  (via C-terminus of  $G\alpha$ ) and the effect on their localization at the surface of the cell membrane which occurs via the N-terminus. All proteins were properly localized at the cell membrane; this is especially noticeable in the case of overexpression of the complete trimer (Fig. 1).  $G\alpha_s$ , investigated as subunit non-interacting with  $D_2R$  as well as with different characteristics, also exhibited proper cellular localization and a similar behavior as  $G\alpha_i$  with reference to the influence of  $G\beta_1\gamma_2$  on localization. The  $G\alpha_s$  subunit was fused with mCitrine or mGFP cloned between the helical and GTPase domains by

replacing amino acids 72–82 with an FP sequence and adding short linkers [42].

The functionality of some of the G proteins prepared in this manner was already verified by other authors. They found that these insertions did not change the properties of the proteins, such as their interaction with adenylyl cyclase, localization at the surface of the cell membrane, or the process of nucleotides exchange [39, 42]. Nevertheless, the activity of all the proteins was investigated by taking into account their ability to inhibit adenylyl cyclase after the activation of  $D_2R$ . Our previous studies have indicated that the differences in the response of  $G\alpha_3$ -mCitrine or  $G\alpha_3$ -mGFP fusion proteins are insignificant. Therefore, only the configurations with  $G\alpha$ -mCitrine were investigated further [34]. For the activation of  $D_2R$ , rotigotine hydrochloride was used as a full agonist, which exhibits an equally functional response as dopamine [43]. Rotigotine is not a selective dopamine  $D_2R$  agonist, but in the present study, the cellular response induced by stimulation with this compound enabled us to observe the differences between the  $G\alpha_i$  subtypes (Fig. 2). It is noteworthy to mention that this agonist also binds efficiently to the dopamine D1-like receptors, which was confirmed by the measurements of cAMP levels. These results are in agreement with observations reported by other research groups [43–45].

The ability of rotigotine to activate  $D_2R$  was confirmed by the measurements of intracellular cAMP levels taken in all the investigated settings (Fig. 2). However, data on the ability of this agonist to inhibit or activate adenylyl cyclase are limited in the literature. Most of the available studies focus on the thermodynamic and kinetic properties associated with binding to the receptor, or the overall pharmacological effect [46–48]. By contrast, in the present study, we analyzed the response of different subtypes of  $G\alpha_i$  and  $G\alpha_s$  by changes in the intracellular cAMP level following the stimulation of cells in which  $D_2R$  and  $G\alpha$  were induced for overexpression. In the case of overexpression of only  $G\alpha_i$  and  $D_2R$ , two  $G\alpha$  subunits were able to inhibit adenylyl cyclase at a statistically significant level ( $G\alpha_2$ ;  $p < 0.001$ ;  $G\alpha_3$ ;  $p < 0.05$ ), except  $G\alpha_1$ . Additionally, as assumed, full  $G\alpha_i$  heterotrimers showed an increased ability to interact with  $D_2R$ , which was indicated by statistically significant differences when the effects of  $G\alpha_i$ - $D_2R$  and  $G\alpha_i\beta_1\gamma_2$ - $D_2R$  interactions were compared. The higher level of  $G\beta_1\gamma_2$  dimer present in cells supported the formation of the whole trimer more efficiently and influenced the behavior of the  $G\alpha_i$  subunits investigated. It is worth noticing that in comparison with control conditions, the differences between the  $G\alpha_i$  subunits diminished upon additional overexpression of  $G\beta_1\gamma_2$  and only comparison between

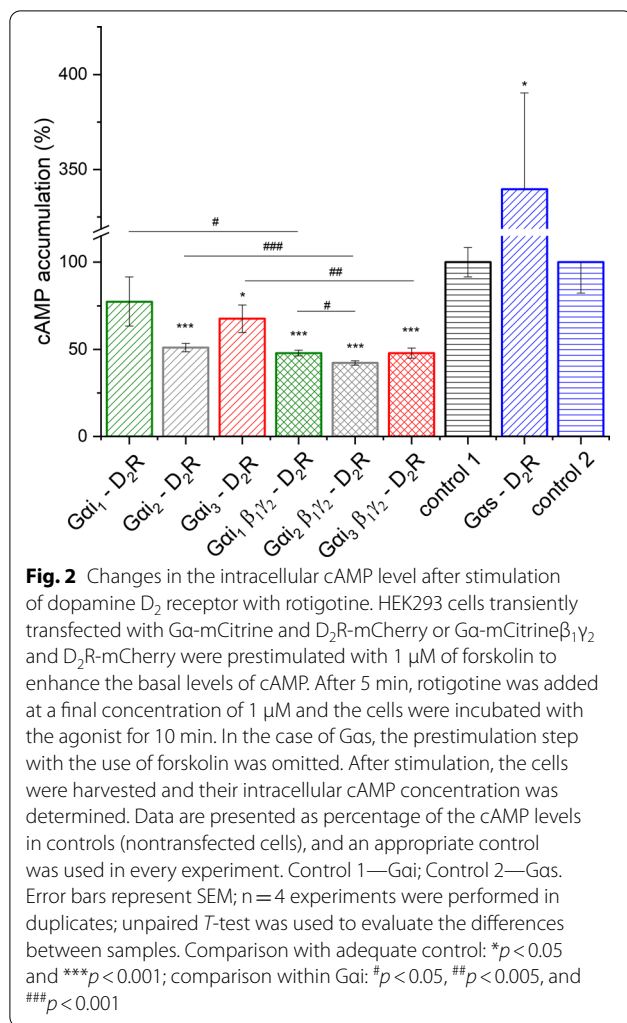


Gαi<sub>1</sub>β<sub>1</sub>γ<sub>2</sub> and Gαi<sub>2</sub>β<sub>1</sub>γ<sub>2</sub> showed significant differences in the cAMP level ( $p < 0.01$ ); in the case of Gαi<sub>3</sub>β<sub>1</sub>γ<sub>2</sub>, such a phenomenon was not observed. The obtained results indicate that Gαi<sub>2</sub> has the most profound influence on the inhibition of adenylyl cyclase, in the case of both overexpression of only Gα subunit or additional overexpression of Gβ<sub>1</sub>γ<sub>2</sub> dimers. These results are in agreement with other studies, which used agonists such as dopamine, quinpirole, or N-n-propylnorapomorphine (NPA) [2, 27, 49, 50]. Moreover, incubation of cells overexpressing Gas and D<sub>2</sub>R with rotigotine confirmed the ability of this agonist to induce the activation of adenylyl cyclase ( $p < 0.05$ ). The ability to increase the cAMP level most probably results from the presence of

other isoforms of adenylyl cyclase which are activated by the Gβγ dimer [51].

#### Nanoscale distribution of Gαi and D<sub>2</sub>R monitored by FLIM-FRET and FRAP in living HEK293 cells

In the present study, we have shown that the FLIM-FRET and FRAP assays can be used to characterize the nanoscale spatial distribution of the closely related Gαi subunits in the plasma membrane, which in turn helped in assessing their role in the regulation of coupling preferences of D<sub>2</sub>R-Gαi proteins. Because of the unique spatial sensitivity, FRET was applied to elucidate the organization of the Gαi subunits and their heterotrimers formed with Gβ<sub>1</sub>γ<sub>2</sub> in the plasma membrane. On



the other hand, the FRAP technique was used to study the lateral dynamics of the investigated proteins in the cellular membrane. FRET was analyzed between the mCitrine-labeled Gai or Gas subunits (energy donor) and the mCherry-labeled D<sub>2</sub>R (energy acceptor). The emission spectrum of mCitrine was shown to overlap with the excitation spectrum of mCherry, making them a suitable donor–acceptor pair for FRET [52]. Following the energy transfer between the donor and the acceptor, the lifetime of mCitrine is shortened. This reduction in the fluorescence lifetime of the donor reflects the molecular proximity between the proteins that are linked to the fluorophores of the donor and acceptor. Thus, the FLIM–FRET technology allowed studying the membrane trafficking of Gai as monomers and heterotrimers when co-expressed with D<sub>2</sub>R.

The fluorescence lifetime histograms obtained for mCitrine (Gai<sub>1</sub>-mCitrine, Gai<sub>2</sub>-mCitrine, Gai<sub>3</sub>-mCitrine, Gas-mCitrine) were fitted with a double-exponential

decay function, and FLIM images showing the apparent lifetime of each pixel were generated. These images and the distribution of lifetimes with and without an acceptor in the HEK293 cells, which was estimated using SymPhoTime software, are shown in Fig. 3a–d. The FLIM images of the cells cotransfected with Gai-mCitrine and D<sub>2</sub>R-mCherry showed a reduction in the apparent lifetime of the donor (change in color toward the blue hues across all pixels), compared to those expressing only Gai-mCitrine. For example, the fluorescence lifetimes of mCitrine in the cells expressing Gai<sub>2</sub>-mCitrine were estimated to be 2.76 ± 0.04 ns (τ<sub>1</sub>) and 3.23 ± 0.03 ns (τ<sub>2</sub>), with the amplitude of each of these lifetimes being approximately 40% and 60%, respectively. In the FRET system (cells additionally expressing D<sub>2</sub>R-mCherry), the donor emission curves were also fitted with the double-exponential decay model. However, shortening of the fluorescence lifetime that can be attributed to FRET was observed only in the case of the short component τ<sub>1</sub>, while the other component (τ<sub>2</sub>) remained almost unchanged. This indicates the involvement of only one donor species characterized by the lifetime τ<sub>1</sub> in the energy transfer (FRETing donor state). Therefore, only the FRETing component was taken into account while calculating the FRET efficiency (Fig. 4b).

In the case of cells expressing Gai<sub>2</sub>-mCitrine or Gai<sub>3</sub>-mCitrine, cotransfection with D<sub>2</sub>R-mCherry significantly reduced the apparent lifetime of mCitrine to 1.93 ± 0.03 or 2.06 ± 0.04 ns, respectively (Fig. 3f, g). By contrast, the lifetime of Gai<sub>1</sub>-mCitrine was decreased only slightly (2.39 ± 0.03 ns) in comparison to the τ<sub>1</sub> estimated for the donor alone (2.48 ± 0.04 ns). The efficiencies of energy transfer between different Gai subunits and D<sub>2</sub>R (Fig. 4b) calculated in the present study indicate that the spatial distribution of even closely related Gai subunits differs. Here, we used Gas subunit (not interacting with D<sub>2</sub>R) as a control, which has been reported to prefer localizing in the membrane region that differs from Gai in lipid composition [53]; however, a significant FRET signal with D<sub>2</sub>R was also detected in this case (Fig. 4b). Combining these data, it can be concluded that dopamine D<sub>2</sub>R can exist in different membrane locations.

The apparent diffusion coefficients of monomeric subunits calculated in the study are summarized in Table 1. The lateral mobility of Gai<sub>1</sub>-mGFP and Gai<sub>3</sub>-mGFP was found to be similar (0.316 ± 0.012 and 0.338 ± 0.022 μm<sup>2</sup> s<sup>-1</sup>, respectively). By contrast, the apparent diffusion coefficient of the Gai<sub>2</sub>-mGFP subunit was much higher (0.474 ± 0.015 μm<sup>2</sup> s<sup>-1</sup>). Interestingly, the diffusion characteristics of both Gai<sub>2</sub>-mGFP and Gai<sub>3</sub>-mGFP were not found to change significantly in the presence of dopamine D<sub>2</sub>R-mCherry at the cell membrane. However, for the Gai<sub>1</sub>-mGFP subunit, mobility

slightly increased ( $0.356 \pm 0.014 \mu\text{m}^2 \text{s}^{-1}$ ). This may have resulted from the competition between the receptor and the  $\text{G}\alpha_1$ -mGFP subunit for the membrane regions [36], which was confirmed by the results of the FRET experiments, with the poor efficiency of FRET between  $\text{G}\alpha_1$ -mGFP and  $\text{D}_2\text{R}$ -mCherry indicating separate membrane localization.

The activation of  $\text{D}_2\text{R}$  with rotigotine did not influence the FRET signal observed between the monomeric  $\text{G}\alpha$  and the agonist-receptor complex. This suggests that even if heterotrimers were formed between  $\text{G}\alpha$ -mCitrine and endogenous  $\text{G}\beta\gamma$  dimers, these complexes had no influence on the measured FRET. On the contrary, in the intracellular cAMP assay, a reduction in the level of cAMP was observed for all  $\text{G}\alpha$  monomers (Fig. 2). This might have been caused, at least partly, by the assembly of an additional heterotrimer complex of  $\text{G}\alpha$ -mCitrine fusion proteins with an endogenous  $\text{G}\beta\gamma$  dimer. However, most cells showed an almost unchanged FRET signal upon receptor activation, which indicates that the concentration of heterotrimers formed with endogenous  $\text{G}\beta\gamma$  dimer remains relatively low. In cells expressing additional  $\text{G}\beta_1\gamma_2$ ,  $\text{D}_2\text{R}$  activation resulted in a significant reduction in the FRET efficiency (Fig. 4b).

Thus, the data obtained from the FLIM-FRET and FRAP assays provide new insights about the location of the closely related  $\text{G}\alpha$  subunits in the plasma membrane: (i) FRAP analysis of fluorescently labeled  $\text{G}\alpha_2$  showed its significantly faster lateral diffusion compared to that of  $\text{G}\alpha_3$  and  $\text{G}\alpha_1$ ; (ii) FRET of fluorescently labeled  $\text{D}_2\text{R}$  with  $\text{G}\alpha_2$  and  $\text{G}\alpha_3$  in the plasma membrane was higher than that with  $\text{G}\alpha_1$ . These together suggest the different distributions of  $\text{G}\alpha$  subunits in the plasma membrane.

### Mapping the organization of $\text{G}\alpha$ heterotrimers in the plasma membrane

FRAP analysis was also performed for all the investigated subunits in the heterotrimeric system (Table 1). For this purpose, the HEK293 cells were cotransfected

with additional vectors encoding  $\text{G}\beta_1$  and  $\text{G}\gamma_2$  subunits to provide an excess of  $\text{G}\beta\gamma$  dimers. As shown earlier, the  $\text{G}\beta\gamma$  dimer was found to modulate the lateral diffusion of a heterotrimeric G protein compared to a monomeric  $\text{G}\alpha$  subunit [34]. In addition, the apparent diffusion coefficients of  $\text{G}\alpha_2$  and  $\text{G}\alpha_3$  with  $\text{G}\beta_1\gamma_2$  complexes were estimated to be substantially higher compared to that of monomers ( $0.526 \pm 0.019$  and  $0.424 \pm 0.014 \mu\text{m}^2 \text{s}^{-1}$ , respectively). However, the presence of the  $\text{G}\beta_1\gamma_2$  dimer had the opposite effect on the mobility of  $\text{G}\alpha_1$  subunit, and the  $D_{app}$  value was found to decrease to  $0.237 \pm 0.010 \mu\text{m}^2 \text{s}^{-1}$ . This observed effect is particularly interesting in the case of  $\text{G}\alpha_1$  and  $\text{G}\alpha_3$  subunits because, as monomers with a high sequence identity, these subunits were characterized by identical lateral mobility.

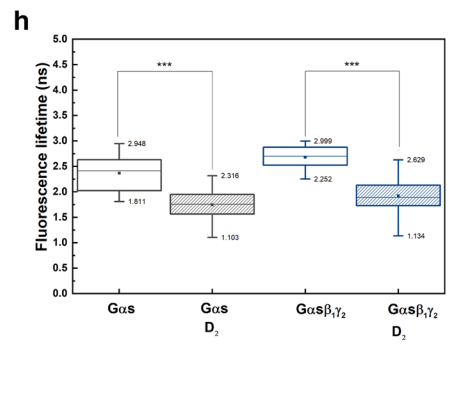
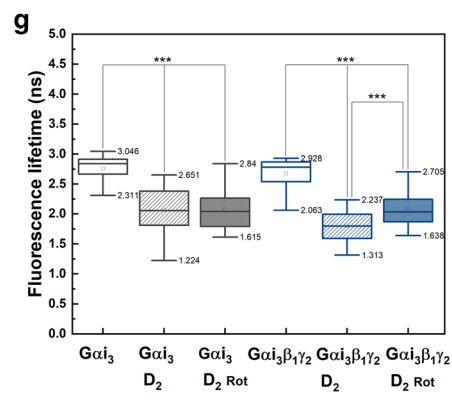
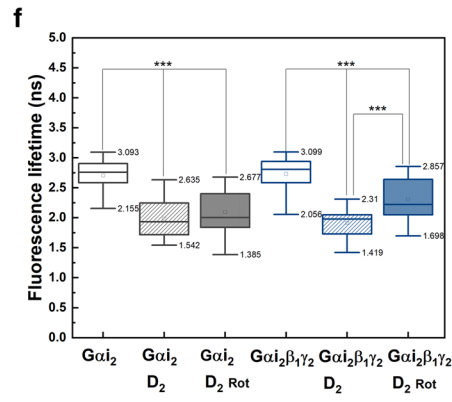
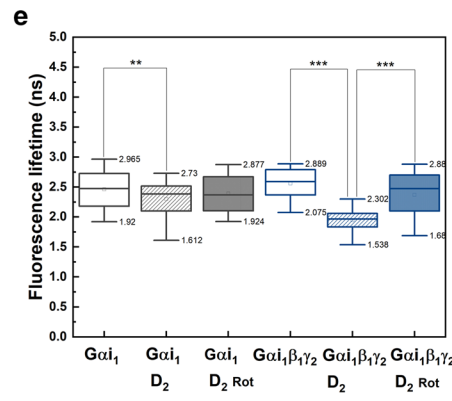
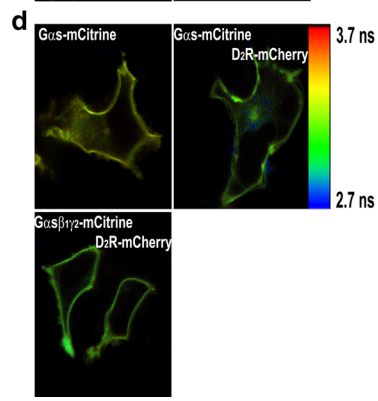
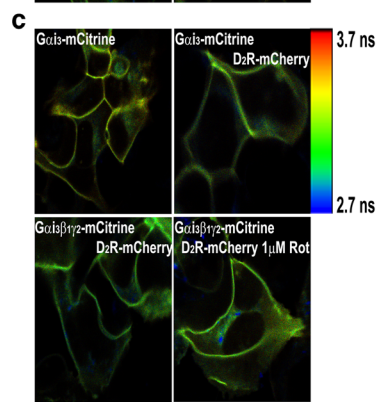
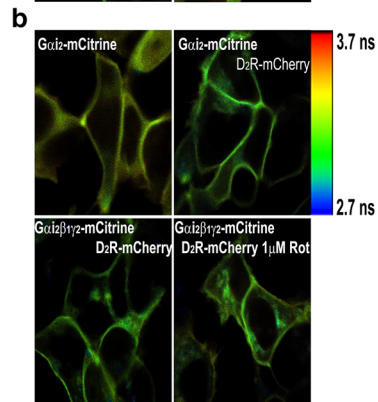
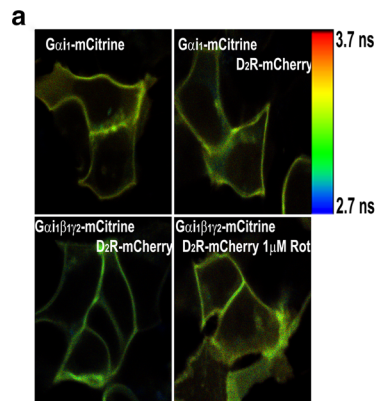
For heterotrimeric  $\text{G}\alpha\beta_1\gamma_2$  complexes, the presence of dopamine  $\text{D}_2\text{R}$  in the cell membrane caused a significant change in the lateral mobility of all the investigated subunits. The biggest difference was observed for the  $\text{G}\alpha_2$  subunit, for which the  $D_{app}$  value declined to  $0.345 \pm 0.013 \mu\text{m}^2 \text{s}^{-1}$ . Such a change in lateral diffusion may have resulted from an effective limitation of mobility to the receptor signaling platform areas such as the raft domains of the plasma membrane [54]. Although, for the  $\text{G}\alpha_1\beta_1\gamma_2$  heterotrimer, a slight increase in  $D_{app}$  was observed ( $0.291 \pm 0.012 \mu\text{m}^2 \text{s}^{-1}$ ) in the presence of  $\text{D}_2\text{R}$ , whereas the mobility of  $\text{G}\alpha_3\beta_1\gamma_2$  slightly decreased in the presence of  $\text{D}_2\text{R}$  compared to the heterotrimer alone ( $0.381 \pm 0.014 \mu\text{m}^2 \text{s}^{-1}$ ). However, it should be noted that in the presence of  $\text{D}_2\text{R}$  the differences in the lateral diffusion rates of the investigated  $\text{G}\alpha$  heterotrimers diminished. This might be due to the colocalization of all heterotrimers with  $\text{D}_2\text{R}$ , which was proved by the FRET measurements.

As shown in Fig. 3e, g, the association of  $\text{G}\alpha_1$  and  $\text{G}\alpha_3$  with  $\text{G}\beta_1\gamma_2$  dimers caused a further reduction in the apparent fluorescence lifetime of mCitrine in the presence of mCherry-fused  $\text{D}_2\text{R}$  (box chart), and thus, there was an increase in the FRET efficiencies. The highest FRET efficiency of  $35.4 \pm 1.6\%$  was detected in the cells co-expressing  $\text{D}_2\text{R}$  and  $\text{G}\alpha_3\beta_1\gamma_2$ , while the

(See figure on next page.)

**Fig. 3** FLIM-FRET results. HEK293 cells were transiently transfected with  $\text{G}\alpha$ -mCitrine alone or both  $\text{D}_2\text{R}$ -mCherry and  $\text{G}\alpha$ -mCitrine (donor and acceptor) with or without  $\text{G}\beta_1\gamma_2$ , or the donor in the presence of the acceptor after treatment with  $1 \mu\text{M}$  rotigotine; mCitrine lifetime was measured: **a**  $\text{G}\alpha_1$ -mCitrine; **b**  $\text{G}\alpha_2$ -mCitrine; **c**  $\text{G}\alpha_3$ -mCitrine; **d** Gas-mCitrine. Fluorescence lifetimes are presented in a continuous pseudo-color scale representing the time values ranging from 2.7 (blue) to 3.7 ns (red). **e-h** Box-and-whisker plots of the fluorescence lifetime  $\tau_1$  of energy donor ( $\text{G}\alpha$ -mCitrine) and donor in the presence of acceptor ( $\text{D}_2\text{R}$ -mCherry) are provided. The median is shown as a line in the box, while the bottom and top boundaries represent the lower and upper quartile, respectively. Statistical significance of the difference in the fluorescence lifetimes of the donor ( $\tau_1$ ) was detected in the absence and presence of the energy acceptor using Mann-Whitney  $U$  test (\*\* $p < 0.005$ , \*\*\* $p < 0.0001$ ).  $\text{G}\alpha_1$ :  $n = 58$ ;  $\text{G}\alpha_1$  and  $\text{G}\beta_1\gamma_2$ :  $n = 40$ ;  $\text{G}\alpha_1$  and  $\text{D}_2\text{R}$  with rotigotine:  $n = 34$ , without rotigotine:  $n = 61$ ;  $\text{G}\alpha_1$  and  $\text{G}\beta_1\gamma_2$  and  $\text{D}_2\text{R}$  with rotigotine:  $n = 26$ , without rotigotine:  $n = 58$ ;  $\text{G}\alpha_2$ :  $n = 49$ ;  $\text{G}\alpha_2$  and  $\text{G}\beta_1\gamma_2$ :  $n = 44$ ;  $\text{G}\alpha_2$  and  $\text{D}_2\text{R}$  with rotigotine:  $n = 41$ , without rotigotine:  $n = 47$ ;  $\text{G}\alpha_2$  and  $\text{G}\beta_1\gamma_2$  and  $\text{D}_2\text{R}$  with rotigotine:  $n = 31$ , without rotigotine:  $n = 46$ ;  $\text{G}\alpha_3$ :  $n = 50$ ;  $\text{G}\alpha_3$  and  $\text{G}\beta_1\gamma_2$ :  $n = 54$ ;  $\text{G}\alpha_3$  and  $\text{D}_2\text{R}$  with rotigotine:  $n = 33$ , without rotigotine:  $n = 68$ ;  $\text{G}\alpha_3$  and  $\text{G}\beta_1\gamma_2$  and  $\text{D}_2\text{R}$  with rotigotine:  $n = 33$ , without rotigotine:  $n = 79$ ; Gas:  $n = 39$ ; Gas and  $\text{G}\beta_1\gamma_2$ :  $n = 39$ ; Gas and  $\text{D}_2\text{R}$ :  $n = 55$ ; Gas and  $\text{G}\beta_1\gamma_2$  and  $\text{D}_2\text{R}$ :  $n = 48$





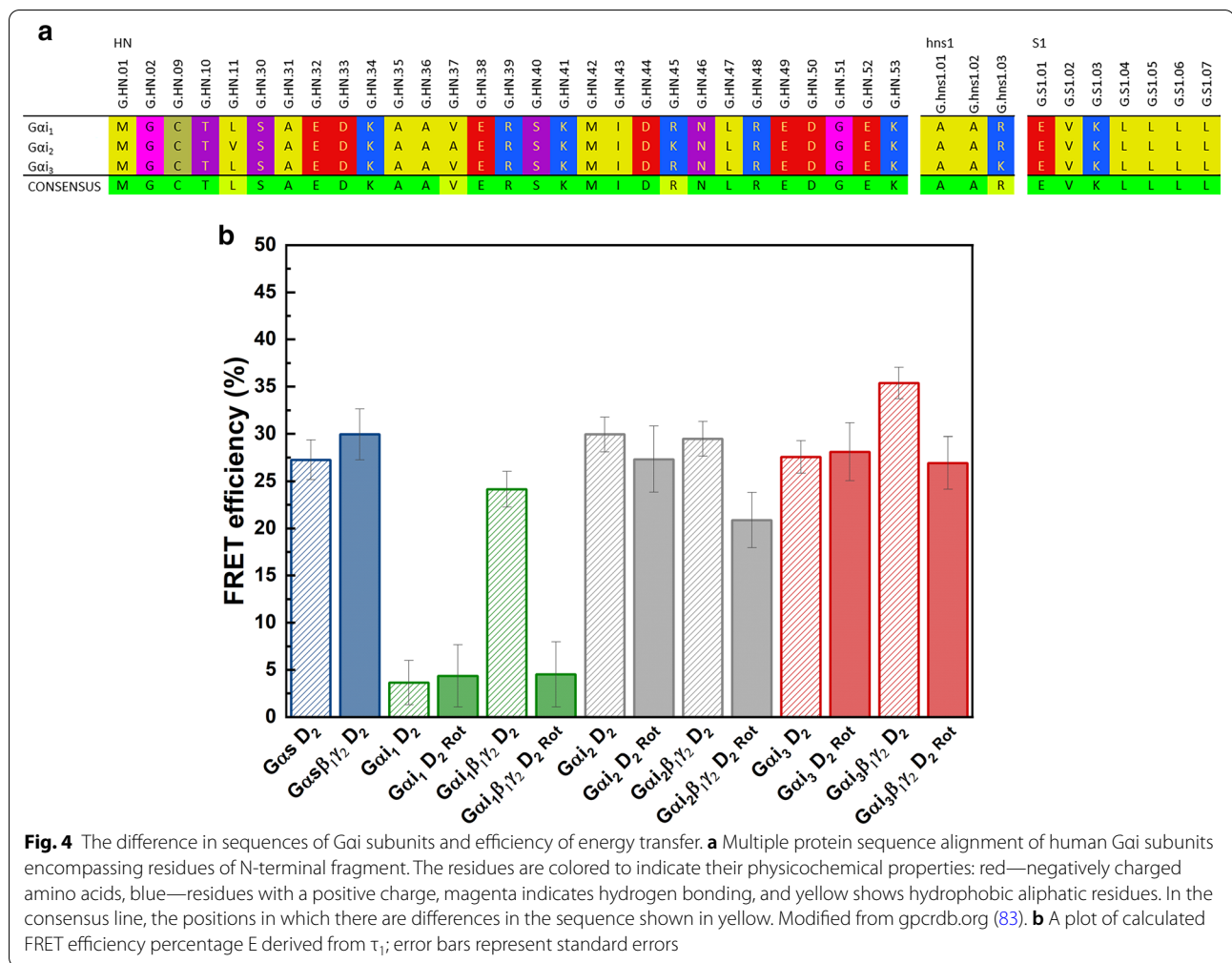


**Fig. 4** The difference in sequences of Gai subunits and efficiency of energy transfer. **a** Multiple protein sequence alignment of human Gai subunits encompassing residues of N-terminal fragment. The residues are colored to indicate their physicochemical properties: red—negatively charged amino acids, blue—residues with a positive charge, magenta indicates hydrogen bonding, and yellow shows hydrophobic aliphatic residues. In the consensus line, the positions in which there are differences in the sequence shown in yellow. Modified from gpcrcdb.org (83). **b** A plot of calculated FRET efficiency percentage E derived from  $\tau_1$ ; error bars represent standard errors

lowest efficiency of 11% was found for the Gai<sub>1</sub>β<sub>1</sub>γ<sub>2</sub> heterotrimer. By contrast, Gai<sub>1</sub>β<sub>1</sub>γ<sub>2</sub> exhibited the same FRET signal with D<sub>2</sub>R as the monomeric Gai<sub>2</sub>. However, the FRET efficiency of this subunit was found to be relatively high. The lifetime of Gai<sub>2</sub>-mCitrine in the heterotrimeric complex was estimated as 2.0 ± 0.03 ns, which amounted to an energy transfer efficiency of 29.5 ± 1.8% (versus 29.9 ± 1.8% with monomeric Gai<sub>2</sub>). These different patterns of changes in the FRET efficiency further point toward the difference in the membrane distribution of distinct Gai subunits and D<sub>2</sub>R. Interestingly, in appropriate FRET pairs, differences were observed in the contribution of the fluorescence decay times for Gai-mCitrine in heterotrimeric complex and the monomeric Gai. The amplitude of the FRETing component ( $\tau_1$ ) decreased to 17% and 25% for Gai<sub>1</sub>β<sub>1</sub>γ<sub>2</sub> and Gai<sub>3</sub>β<sub>1</sub>γ<sub>2</sub>, respectively, whereas it remained at the same level for Gai<sub>2</sub>β<sub>1</sub>γ<sub>2</sub>, similar to that calculated for the D<sub>2</sub>R–Gai<sub>2</sub> pair. The simplest explanation that could be provided for this effect is that the subpopulations of Gai<sub>1</sub> and Gai<sub>3</sub>, for which the

energy transfer to D<sub>2</sub>R-mCherry was reduced, relocate within the membrane upon the formation of the heterotrimeric complex. Thus, based on the FLIM data, it can be concluded that the receptor and heterotrimeric G protein in the basal state (before receptor activation) localize at the cell membrane within the same area (signaling platform), promoting signal transduction.

FRET analysis revealed that all the Gai heterotrimers responded to the agonist rotigotine. The activation of D<sub>2</sub>R with rotigotine caused a significant reduction in the FRET efficiency in the case of all heterotrimers (Fig. 4b). The most pronounced decrease was observed for Gai<sub>1</sub>β<sub>1</sub>γ<sub>2</sub>, while the lowest decrease was noted for Gai<sub>2</sub>β<sub>1</sub>γ<sub>2</sub>. However, the difference observed in the FRET signal between the G protein and D<sub>2</sub>R before and after receptor stimulation cannot be interpreted as the magnitude of the rotigotine effect. D<sub>2</sub>R activation by agonist leads to the activation of G protein, which is accompanied by the dissociation of Gα from the Gβγ dimer, followed by Gα translocation within the plasma membrane

**Table 1 Lateral diffusion characteristics of Gα subunits in HEK293 cells in the presence of Gβ<sub>1</sub>γ<sub>2</sub> and/or dopamine D<sub>2</sub> receptor**

|   | $D_{app}$<br>( $\mu\text{m}^2 \text{s}^{-1}$ ) | $M_f$<br>(%) | N   |
|---|--|--------------|-----|
| Gas <sup>a</sup>  | 0.130 ± 0.004                                  | 84.5 ± 1.5   | 49  |
| Gas Gβ <sub>1</sub> γ <sub>2</sub> <sup>b</sup>                 | 0.246 ± 0.009                                  | 92.4 ± 0.8   | 143 |
| Gas D <sub>2</sub> R  | 0.232 ± 0.009                                  | 89.0 ± 1.0   | 88  |
| Gasβ <sub>1</sub> γ <sub>2</sub> D <sub>2</sub> R               | 0.245 ± 0.009                                  | 90.6 ± 1.1   | 110 |
| Gai <sub>1</sub>  | 0.316 ± 0.012                                  | 91.8 ± 1.4   | 55  |
| Gai <sub>1</sub> Gβ <sub>1</sub> γ <sub>2</sub>                 | 0.237 ± 0.010                                  | 88.2 ± 1.6   | 53  |
| Gai <sub>1</sub> D <sub>2</sub> R                               | 0.356 ± 0.014                                  | 92.2 ± 1.4   | 45  |
| Gai <sub>1</sub> β <sub>1</sub> γ <sub>2</sub> D <sub>2</sub> R | 0.291 ± 0.012                                  | 91.0 ± 1.2   | 60  |
| Gai <sub>2</sub>  | 0.474 ± 0.015                                  | 95.2 ± 0.7   | 120 |
| Gai <sub>2</sub> Gβ <sub>1</sub> γ <sub>2</sub>                 | 0.526 ± 0.019                                  | 94.1 ± 1.3   | 50  |
| Gai <sub>2</sub> D <sub>2</sub> R                               | 0.467 ± 0.020                                  | 93.1 ± 1.4   | 58  |
| Gai <sub>2</sub> β <sub>1</sub> γ <sub>2</sub> D <sub>2</sub> R | 0.345 ± 0.013                                  | 90.9 ± 1.3   | 60  |
| Gai <sub>3</sub> <sup>a</sup>                                   | 0.338 ± 0.022                                  | 94.2 ± 1.7   | 34  |
| Gai <sub>3</sub> Gβ <sub>1</sub> γ <sub>2</sub> <sup>b</sup>    | 0.424 ± 0.014                                  | 93.5 ± 0.9   | 66  |
| Gai <sub>3</sub> D <sub>2</sub> R                               | 0.358 ± 0.016                                  | 90.1 ± 1.5   | 60  |
| Gai <sub>3</sub> β <sub>1</sub> γ <sub>2</sub> D <sub>2</sub> R | 0.381 ± 0.014                                  | 91.0 ± 1.4   | 50  |

In the experiments where the co-expression took place, the diffusion of Gα subunits was measured. Values represent the mean ± S.E.M

$D_{app}$ —apparent diffusion coefficient,  $M_f$ —mobile fraction

<sup>a</sup> Data from Ref. [40]

<sup>b</sup> Data from Ref. [34]

and the internalization of the receptor. Because the complexes formed between the agonist-bound D<sub>2</sub>R and the G proteins have short lifetimes [55], which are off the time scale of the FLIM measurement, the recorded FLIM signal comes dominantly from the further steps of the signaling cascade. Thus, the FRET signal obtained after receptor stimulation should be compared to the value of FRET between monomeric Gai and D<sub>2</sub>R. According to which the most pronounced effect of rotigotine was observed for Gai<sub>2</sub>β<sub>1</sub>γ<sub>2</sub>.

### Discussion

Dopamine is a neurotransmitter that plays a critical role in controlling movement, cognition, and emotion. Dopamine receptors are expressed in neurons of the nigrostriatal pathway (motor-related), the mesolimbic-cortical pathway (reward system, emotional control) and tuberoinfundibular system [56]. Peripheral dopamine neurons are involved in renal and cardiovascular functions, and immune regulation. Dysfunction of dopaminergic pathways play an essential role in the pathophysiology of Parkinson’s disease, schizophrenia, mood disorders, attention-deficit disorder, Huntington’s disease, Tourette’s syndrome, Tardive dyskinesia, and other disorders. Therefore, insight into the selectivity of signal

transduction between the dopamine receptor and G proteins is crucial for understanding of current therapies and development of new treatments. Interestingly, 21.9% of all GPCRs couple exclusively to the Gai/o subfamily, another 5% couple to Gai/o and of other G subfamilies [57]. All these receptors may couple differentially among various Gai and Gao isoforms, and individually prefer one specific isoform to the others [58–60].

The structural details behind the selectivity of receptor–G protein activation remain unclear and are an important subject of biochemical and biophysical studies [17, 23, 61, 62]. Studies dealing with the Gas, Gai, and Gαq families have shown their direct roles in regulating the levels of the secondary messenger and have provided substantial insight into the GPCR–G protein interface [63–65]. Despite that there is a plethora of data regarding the coupling specificity of various GPCRs, only a little is known about the potential receptor selectivity between the closely related members of the G protein families. In the present study, we have focused on the functional selectivity of dopamine D<sub>2</sub>R toward the Gα<sub>11</sub>, Gα<sub>12</sub>, and Gα<sub>13</sub> subunits, and analyzed whether the organization of Gai heterotrimers in the plasma membrane can influence D<sub>2</sub>R signaling. This is particularly interesting in light of the current understanding of the complexity observed with the structural and functional organization of the cell membranes. The different lipid species present in membranes influence their properties, including the formation of membrane domains, as well as induce changes in the activity and density of the membrane proteins. However, it is not known whether the organization of G proteins in the plasma membrane influences their coupling with D<sub>2</sub>R or whether it might be one of the determinants of their coupling selectivity. Since it has been reported that there are differences in the plasma membrane targeting and trafficking pathways of the G proteins composed of Gα subunits belonging to different subfamilies, it is, therefore, reasonable to also evaluate the behavior of heterotrimers composed of closely related Gai in the membranes, especially taking into account the already existing data [34, 53, 66, 67].

The membrane-binding area of Gα is limited to two sites on the surface of the protein and the membrane [67]. Its most critical membrane-binding determinant is the lipid anchors in conjunction with a polybasic motif at the N-terminus [66, 68, 69]. Depending on the specific subclass, the Gα subunits are palmitoylated and mostly myristoylated [70, 71]. All the Gai subunits are N-myristoylated and S-palmitoylated, and the amino acid identity among them is high: Gai<sub>1</sub> and Gai<sub>3</sub> share a sequence identity of 94%, whereas Gai<sub>2</sub> has a lower identity of 87.5% and 85.5% to Gai<sub>1</sub> and Gai<sub>3</sub>, respectively. We found two differences between

the  $G\alpha_i$  subunits in the positively charged motif at the N-terminus, which appear to be relevant (Fig. 4a). The first one concerns the position 21 where an R residue is present in  $G\alpha_i_3$  and  $G\alpha_i_1$ , while a K residue is present in  $G\alpha_i_2$ . An additional substitution is found at position 32 of  $G\alpha_i_3$ , where K is present in the place of R in  $G\alpha_i_1$  and  $G\alpha_i_2$ . However, when comparing the diffusion coefficients of  $G\alpha_i_3$  and  $G\alpha_i_1$ , this position seems to be of lower importance in attaching  $G\alpha_i$  to the membrane. Even if these substitutions did not appear to be significant, as they had no effect on the charge of the amino acid residues, it was assumed that they affect the interactions of  $G\alpha_i$  with the membrane and might also influence the efficiency of translocation of  $G\alpha$  within the membrane. Our diffusion data suggest that the N-terminal residues of the  $G\alpha$  function as an essential signal to ensure the correct localization of the  $G\alpha_i$  subunits at the plasma membrane.

The sequence differences in the polybasic motif between the  $G\alpha_i$  subunits seemed to correlate well with the differences in their lateral diffusion coefficients detected by the FRAP experiments. The diffusion coefficient of the subunits increases in the following order:  $G\alpha_i_1 \leq G\alpha_i_3 < G\alpha_i_2$ . Our data strongly suggest that the presence of the cluster of positively charged amino acids in the N-terminus of  $G\alpha_i$  contributes to the membrane targeting of  $G\alpha$ , thus strengthening its affinity to the plasma membrane. The reduced membrane mobility of  $G\alpha_i_1$  corresponds to the presence of a larger number of R residues in the polybasic motif. Both K and R function as basic residues; however, they differ in their geometric structure and possible interactions. Compared to the K residue, the R residue forms a higher number of electrostatic interactions, such as salt-bridges and hydrogen bonds, so it presumably results in stronger interactions than those generated by the lysine residue [72, 73]. The interactions that are observed for the positively charged residues include hydrogen bonds to the phosphate groups of phospholipids and electrostatic interactions to the negatively charged lipids at the cytosolic surface of the membrane [74]. Together, these interactions might cause retention of the positively charged residues on the cytoplasmic face of the membrane, slowing down the membrane mobility of the protein. In line with this hypothesis, in the present study, the  $G\alpha_s$  subunit, which possesses a higher number of positively charged residues in the polybasic motif, showed the slowest membrane mobility among all the investigated  $G\alpha$  subunits.

On the other hand, the slower rate of lateral diffusion observed for  $G\alpha$  indicates that molecular motion is transiently confined, and such a protein resides within a particular region for a longer period of time. This in turn could enhance the FRET signal—in this case, the energy

transfer between  $D_2R$  and the slowest diffusing  $G\alpha_i$  subunit (assuming a similar distribution for all the  $G\alpha_i$  subunits across the membrane). As mentioned above, the FRET technique was applied to assess the trafficking of  $G\alpha_i$  as monomers and heterotrimers when co-expressed with dopamine  $D_2R$  and to analyze the corresponding changes in their relative membrane localization. Interestingly, we detected that the resonance energy transfer between  $D_2R$  and the slowest diffusing  $G\alpha_i$  subunit— $G\alpha_i_1$ —had the lowest efficiency (almost none). The highest FRET signal was observed for the fastest diffusing  $G\alpha_i_2$ , while a slightly less efficient signal was recorded for  $G\alpha_i_3$  (diffusion rates comparable to  $G\alpha_i_1$ ) and  $G\alpha_s$  (the slowest diffusion rate). These results indicate that the sequestration of  $G\alpha$  subunits, even those belonging to the same  $G\alpha_i$  subfamily, in the plasma membrane may also vary.

In our earlier work, which investigated the distribution of  $G\alpha_s$  and  $G\alpha_i_3$  in the plasma membrane, we observed that these proteins were localized in different types of specific membrane domains [53]. It was found that the  $G\alpha_s$  subunits preferred solid-like domains (insensitive to cholesterol, with a structure or composition of lipid rafts), while the  $G\alpha_i_3$  subunit preferred the more fluid regions of the membrane and detergent-resistant domains such as lipid rafts. This suggests that distinct protein acylation may act as a signal for recruitment or retention into particular membrane regions/domains containing specific lipids. As already mentioned, despite that all the  $G\alpha_i$  subunits had the same lipid anchors, the difference in the sequence of the polybasic region (for example, the presence of additional R residues) has an impact on the lipid preference and membrane localization of the subunits. A similar value of apparent diffusion coefficient observed for  $G\alpha_i_1$  and  $G\alpha_i_3$  in this study suggests their similar membrane localization. Therefore, it is tempting to conclude that  $G\alpha_i_1$  also prefers detergent-resistant and cholesterol-dependent membrane domains (i.e. Lo-like domains) in the plasma membrane. However, the FRET data do not support this interpretation (as different FRET efficiency was estimated for the pairs  $D_2R$ – $G\alpha_i_1$  and  $D_2R$ – $G\alpha_i_3$ ). The main limitation of the FRAP studies is that it does not provide detailed information about where the species are present and the subpopulations in different locations cannot be simply identified. Another important aspect that needs to be considered is the nature of the interaction of the R residue with the membrane, as in some cases it leads to a local distortion of the bilayer around proteins [74]. This distortion is manifested in a high level of local water penetration inside the membrane, and can lead to a decrease in the thickness of the bilayer as well as affect the long-range interactions. We cannot rule out that the lower FRET

signal observed between  $D_2R$  and  $G\alpha_i$  could result from the local deformation of the membrane induced by  $G\alpha_i$ , which affects the distribution and density of  $D_2R$  in such an area in the membrane. This scenario is quite probable since the N-terminus of  $G\alpha_i$  is arginine-rich, and the dopamine  $D_2R$  is broadly distributed throughout the cell membrane, as supported by our FRET results. It has been shown by Sharma et al. that  $D_2R$  exists in both detergent-soluble and detergent-insoluble fractions of the plasma membrane [36]. The similar plasma membrane localization of the  $G\alpha_i$  and  $G\alpha_3$  subunits cannot be excluded; however, faster diffusion of  $G\alpha_2$  indicates that this subunit is localized within the membrane area which is composed of different types of lipids, a more fluid membrane area, and rich in  $D_2R$ , as suggested by our FRET data.

As reported in our previous work, the diffusion of the  $G\alpha$  and  $G\alpha_3$  subunits speeds up upon the formation of heterotrimer [34, 40]. The  $G\beta\gamma$  dimer is responsible for the rapid relocation of  $G\alpha$  from the lamellar membrane region where it resides as a monomer [67]. As expected, the membrane mobility of  $G\alpha_2\beta_1\gamma_2$  and  $G\alpha_3\beta_1\gamma_2$  changed in a similar way. The association of  $G\beta_1\gamma_2$  with the GDP-bound  $G\alpha_2$  or  $G\alpha_3$  caused the G proteins to relocate into the more fluid membrane regions (the diffusion rate increased despite the increase in the molecular weight of the complex). However, an opposite behavior was observed for  $G\alpha_1$ . In the case of this subunit, when the trimer was formed, its membrane mobility slowed down the diffusion rate. This implies that—in contrast to  $G\alpha_2$  and  $G\alpha_3$ — $G\alpha_1$  in the heterotrimer complex did not change its lipid environment or changed it only slightly (the formation of heterotrimers by  $G\alpha_1$  did not involve the translocation of this protein into a more fluid region in the membrane as noted for the rest of the  $G\alpha$  subunits). Alternatively, the observed slow-down of the heterotrimer diffusion could be a sustained effect of the structural perturbations of the lipid bilayers that were caused by the N-terminus of  $G\alpha_1$ , which also affected the diffusion of the full heterotrimeric complex. To clearly discriminate between these possibilities, structural *in vitro* studies in a model system (purified proteins and lipid bilayers) are required. However, the impact of the  $G\beta_1\gamma_2$  dimer on the membrane distribution of the complete complex of  $G\alpha_1\beta_1\gamma_2$  is unquestionable, as was indicated by the significant FRET signal between the complete heterotrimer and  $D_2R$  compared to the almost undetectable signal of the monomeric  $G\alpha_1$ . Previous studies of fluorescence and electron paramagnetic resonance have also pointed out that the N-terminus of  $G\alpha_1$  undergoes a conformational change upon  $G\beta\gamma$  binding and activation [75].

Taken together, this new experimental evidence strengthens our earlier hypothesis that the  $G\beta\gamma$  dimer

alone does not define the affinity or specificity of the complete heterotrimer toward the membrane lipid phase [34]. In general, the distinct heterotrimeric combinations showed differences in their mobility characteristics (Table 1). Therefore, the interplay between the  $G\beta\gamma$  and  $G\alpha$  subunits is critical for controlling the trafficking of the complete G protein heterotrimer. Moreover, we found that for some heterotrimers,  $G\alpha$  acts as a crucial modulator of the membrane localization. These findings appear to be in contradiction with the previously published results of the nuclear magnetic resonance-based studies (on purified proteins and liposomes), suggesting that only  $G\beta\gamma$  dimer is responsible for the cellular localization of the heterotrimeric  $G\alpha_1$  proteins, thereby masking the lamellar membrane affinity of  $G\alpha_1$  [67].

Besides the observed changes in diffusion rates, the  $G\beta_1\gamma_2$ -dependent translocation of the  $G\alpha_1$  and  $G\alpha_3$  subunits also induced an increase in the FRET efficiency. The simplest explanation that can be given for this phenomenon is that the heterotrimers are localized within the  $D_2R$ -rich membrane fraction and are waiting for the agonist-activated receptor. By contrast, we found that the FRET signal between  $G\alpha_2\beta_1\gamma_2$  and  $D_2R$  remained at the same level as that calculated for the  $D_2R$ – $G\alpha_2$  pair. Since the monomeric  $G\alpha_2$  is located in the  $D_2R$ -rich membrane region, it is most likely that its spatial distribution undergoes only a slight change upon heterotrimer formation. Our data are in general agreement with the results published by Sharma et al. [36] who observed that the majority of the plasma membrane-expressed population of  $D_2R$  was located within the detergent-resistant structures that do not correspond to classical lipid rafts. Treatment with an agonist led to the loss of both the detergent-soluble and detergent-resistant  $D_2R$  fractions; however, the loss of detergent-resistant fraction was significantly greater.

In the present study, we found that the use of an anti-parkinsonian drug, rotigotine, as a  $D_2R$  agonist led to the inhibition of cAMP production and noticed a difference in the coupling selectivity of heterotrimers. The order of rotigotine potency ( $G\alpha_2 > G\alpha_3 = G\alpha_1$ ) observed in the FRET experiments remains in general agreement with the results shown by direct measurement of the level of intracellular cAMP. Because the complexes formed between agonist-bound  $D_2R$  and G proteins have short lives, the time-resolution of the FRET measurements allowed detecting only the further steps in the signaling cascade: dissociation of  $G\alpha$  from the trimer complex, followed by its relocation within the plasma membrane and receptor internalization. All these processes together were manifested as a decrease in the FRET efficiency, as compared to the basal signal (FRET for  $D_2R$ – $G\alpha$  pair). It is noteworthy that in several earlier reports,  $G\alpha_2$  was

also indicated as selective toward D<sub>2</sub>R, causing maximal inhibition of adenylate cyclase [26, 76, 77]. However, the experimental data imply that the coupling selectivity of G $\alpha$ i is regulated by the agonist-activated conformation of D<sub>2</sub>R. For example, stimulation of D<sub>2</sub>R with R(+)-3-PPP hydrochloride caused preferential coupling to G $\alpha$ i<sub>3</sub> rather than G $\alpha$ i<sub>1</sub> or G $\alpha$ i<sub>2</sub> [25]. The C-terminal G $\alpha$ , as well as the movement magnitude of the sixth transmembrane helix of activated receptor, which varies from one receptor to another, has been predicted to be the main modulator of the selectivity of the G protein subtypes. Regarding the G $\alpha$ i subunits, the sequence of C-terminal helix is almost identical for all proteins (two substitutions in G $\alpha$ i<sub>3</sub>: 350D/E, 354F/Y). Furthermore, neither the amino acid sequences of  $\beta$ 2– $\beta$ 3 loop nor the  $\beta$ 6 sheet in the Ras-like domain—additional residues predicted as selectivity determinants—show any significant differences (one substitution in G $\alpha$ i<sub>3</sub>, 195H/Y) [15, 23]. This clearly indicates that there must be other selectivity determinants for the coupling of G $\alpha$ i heterotrimers. Our data support the new idea that membrane location can serve as an important selectivity determinant of downstream signaling. Considering that the ligated receptors might be clustered [78, 79] for longer durations within the given domains in the cell membrane, which also contain appropriate G protein, it seems likely that this combination fine-tunes the sensitivity and specificity of a given signaling pathway.

## Conclusions

The concept of rapid translocation of the G $\alpha$  monomers after dissociation from the G $\beta\gamma$  dimer and their localization to the lamellar structures, where they interact with effector molecules, is widely accepted and has also been confirmed by numerous studies [6, 80, 81]. The model of membrane localization-dependent signaling by G protein has been proposed over a decade ago. However, since then, the knowledge of membrane organization and functioning has significantly evolved [54, 82]. Therefore, some aspects of this model require revision. For instance, all the monomeric G $\alpha$ i subunits are considered as identical in terms of their membrane coupling, and it has been postulated that they localize to the same type of membrane structures—lipid raft domains [31, 32]. In fact, as proved in the present study, even closely related subunits of G $\alpha$ i differ in their membrane trafficking properties that influence their signaling. The interactions between lipids and proteins seem to be crucial in GPCR-dependent cell signaling due to their functional organization in specific membrane domains, and should therefore be taken into account as one of the selectivity determinants of G protein coupling.

## Supplementary Information

The online version contains supplementary material available at <https://doi.org/10.1186/s12964-020-00685-9>.

**Additional file 1.** Supplemental RT-qPCR experiments.

### Abbreviations

GPCR: G protein-coupled receptor; D<sub>2</sub>R: Dopamine D<sub>2</sub> receptor; FRAP: Fluorescence recovery after photobleaching; FRET: Fluorescence resonance energy transfer; FLIM: Fluorescence-lifetime imaging microscopy; HEK293: Human embryonic kidney 293 cells; cAMP: 3',5'-Cyclic adenosine monophosphate; GTP: Guanosine-5'-triphosphate; GDP: Guanosine diphosphate; ICL: Intracellular loops; TM: Transmembrane helix; RGS: Regulators of G protein signaling; AGS: Receptor-independent activators of G-protein; PCR: Polymerase chain reaction; mGFP: Monomeric Green Fluorescent Protein; FP: Fluorescent protein; MEM: Minimum essential medium; FBS: Fetal bovine serum; NPA: N-n-propylnorapomorphine; D<sub>app</sub>: Apparent diffusion coefficient; M<sub>f</sub>: Mobile fraction.

### Authors' contributions

Conceptualization: A.P. and P.M. Formal analysis: A.P., P.M. and B.R. Funding acquisition: A.P. Investigation: Genetics constructs: P.M., B.R. FRAP experiments: P.M. FLIM–FRET experiments: A.P. and B.R. cAMP production experiments: B.R. RT-qPCR experiments: E.B. Project administration: A.P. Visualization: P.M., A.P. Writing—original draft: A.P., B.R. and P.M. Writing—review and editing: A.P., M.D.-W., P.M. and B.R. All authors read and approved the final manuscript.

### Funding

This work was supported by a grant awarded by the Polish National Center for Science (NCN, no. 2016/23/B/NZ1/00530). The open-access publication of this article was funded by the Priority Research Area BioS under the program "Excellence Initiative—Research University" at the Jagiellonian University in Kraków.

### Availability of data and materials

The datasets generated during and/or analysed during the current study are available from the corresponding author on reasonable request.

### Ethics approval and consent to participate

Not applicable.

### Consent for publication

Not applicable.

### Competing interests

The authors declare that there is no competing interests.

Received: 27 April 2020 Accepted: 10 November 2020

Published online: 11 December 2020

## References

1. Sriram K, Insel PA. GPCRs as targets for approved drugs: How many targets and how many drugs? *Mol Pharmacol*. 2018;93:251–8.
2. Neve KA, Seamans JK, Trantham-Davidson H. Dopamine Receptor Signaling. *J Recept Signal Transduct Res*. 2004;24:3.
3. Beaulieu J-M, Gainetdinov RR. The physiology, signaling, and pharmacology of dopamine receptors. *Pharmacol Rev*. 2011;63:1.
4. Syrovatkina V, Alegre KO, Dey R, Huang XY. Regulation, signaling, and physiological functions of G-proteins. *J Mol Biol*. 2016;428:19.
5. Sokolov M, Lyubarsky AL, Strissel KJ, Savchenko AB, Govardovskii VI, Pugh EN, et al. Massive light-driven translocation of transducin between the two major compartments of rod cells: a novel mechanism of light adaptation. *Neuron*. 2002;34:1.
6. Vögler O, Barceló JM, Ribas C, Escrivá PV. Membrane interactions of G proteins and other related proteins. *Biochim Biophys Acta Biomembr*. 2008;1778:7–8.

7. Van Keulen SC, Rothlisberger U. Effect of N-terminal myristoylation on the active conformation of Gai1-GTP. *Biochemistry*. 2017;56:1.
8. Loisel TP, Ansanay H, Adam L, Marullo S, Seifert R, Lagacé M, et al. Activation of the  $\beta_2$ -adrenergic receptor-Ga(s) complex leads to rapid depalmitoylation and inhibition of repalmitoylation of both the receptor and Ga(s). *J Biol Chem*. 1999;274:43.
9. Degtyarev MY, Spiegel AM, Jones TLZ. Palmitoylation of a G protein  $\alpha(i)$  subunit requires membrane localization not myristoylation. *J Biol Chem*. 1994;269:49.
10. Moreira IS. Structural features of the G-protein/GPCR interactions. *Biochem Biophys Acta*. 2014;1840:1.
11. Baltoumas F, Theodoropoulou MC, Hamodrakas SJ. Interactions of the  $\alpha$ -subunits of heterotrimeric G-proteins with GPCRs, effectors and RGS proteins: a critical review and analysis of interacting surfaces, conformational shifts, structural diversity and electrostatic potentials. *J Struct Biol*. 2013;182:3.
12. Sjöstedt E, Zhong W, Fagerberg L, Carlsson M, Mitsios N, Adori C, et al. An atlas of the protein-coding genes in the human, pig, and mouse brain. *Science*. 2020;367:6482.
13. Mahoney JP, Sunahara RK. Mechanistic insights into GPCR-G protein interactions. *Curr Opin Struct Biol*. 2016;41:247–54.
14. Mnpotra JS, Qiao Z, Cai J, Lynch DL, Grossfield A, Leioatts N, et al. Structural basis of G protein-coupled receptor-Gi protein interaction: formation of the cannabinoid CB2 receptor-Gi protein complex. *J Biol Chem*. 2014;289:29.
15. Flock T, Hauser AS, Lund N, Gloriam DE, Balaji S, Babu MM. Selectivity determinants of GPCR-G protein binding. *Nature*. 2017;545:7654.
16. Inoue A, Raimondi F, Kadji FMN, Singh G, Kishi T, Uwamizu A, et al. Illuminating G-protein-coupling selectivity of GPCRs. *Cell*. 2019;177:7.
17. Okashah N, Wan Q, Ghosh S, Sandhu M, Inoue A, Vaidehi N, et al. Variable G protein determinants of GPCR coupling selectivity. *Proc Natl Acad Sci USA*. 2019;116:24.
18. Venkatakrishnan AJ, Deupi X, Lebon G, Heydenreich FM, Flock T, Miljus T, et al. Diverse activation pathways in class A GPCRs converge near the G-protein-coupling region. *Nature*. 2016;536:7617.
19. Glukhova A, Draper-Joyce CJ, Sunahara RK, Christopoulos A, Wootten D, Sexton PM. Rules of engagement: GPCRs and G Proteins. *ACS Pharmacol Transl Sci*. 2018;1:2.
20. Blahos J, Fischer T, Brabet I, Stauffer D, Rovelli G, Bockaert J, et al. A novel site on the Ga-protein that recognizes heptahelical receptors. *J Biol Chem*. 2001;276:5.
21. Sato T, Matsukawa M, Mizutani Y, Iijima T, Matsumura H. Initial, transient, and specific interaction between G protein-coupled receptor and target G protein in parallel signal processing: a case of olfactory discrimination of cancer-induced odors. *Med Res Arch*. 2018;6:9.
22. Calebiro D, Jobin ML. Hot spots for GPCR signaling: lessons from single-molecule microscopy. *Curr Opin Cell Biol*. 2019;57:57–63.
23. Van Eps N, Altenbach C, Caro LN, Latorraca NR, Hollingsworth SA, Dror RO, et al. Gi- and Gs-coupled GPCRs show different modes of G-protein binding. *Proc Natl Acad Sci USA*. 2018;115:10.
24. Masuho I, Ostrovskaya O, Kramer GM, Jones CD, Xie KMK. Distinct profiles of functional discrimination among G proteins determine the actions of G protein-coupled receptors. *Physiol Behav*. 2015;176:1.
25. Gazi L, Nickolls SA, Strange PG. Functional coupling of the human dopamine D2 receptor with Ga i1, Ga i2, Ga i3 and Ga o G proteins: evidence for agonist regulation of G protein selectivity. *Br J Pharmacol*. 2003;138:5.
26. Senogless E, Spiegel M, Caron G. Specificity of receptor-G protein interactions. 1990;265:8.
27. Jiang M, Spicher K, Boulay G, Wang Y, Birnbaumer L. Most central nervous system D2 dopamine receptors are coupled to their effectors by Go. *Proc Natl Acad Sci USA*. 2001;98:6.
28. Garcia-Parajo MF, Cambi A, Torreno-Pina JA, Thompson N, Jacobson K. Nanoclustering as a dominant feature of plasma membrane organization. *J Cell Sci*. 2014;127:23.
29. Guigas G, Weiss M. Effects of protein crowding on membrane systems. *Biochim Biophys Acta Biomembr*. 2016;1858:10.
30. Oh P, Schnitzer JE. Segregation of heterotrimeric G proteins in cell surface microdomains. G(q) binds caveolin to concentrate in caveolae, whereas G(i) and G(s) target lipid rafts by default. *Mol Biol Cell*. 2001;12:3.
31. Moffett S, Brown DA, Linder ME. Lipid-dependent targeting of G proteins into rafts. *J Biol Chem*. 2000;275:3.
32. Oh P, Schnitzer JE. Segregation of heterotrimeric G proteins in cell surface microdomains: GQ binds caveolin to concentrate in caveolae, whereas gi and GS target lipid rafts by default. *Mol Biol Cell*. 2001;12:3.
33. Evanko DS, Thiyagarajan MM, Siderovski DP, Wedegaertner PB. G $\beta\gamma$  isoforms selectively rescue plasma membrane localization and palmitoylation of mutant Gas and G $\alpha_q$ . *J Biol Chem*. 2001;276:26.
34. Mystek P, Rysiewicz B, Gregrowicz J, Dziedzicka-Wasylewska M, Polit A. Gy and Ga identity dictate a G-protein heterotrimer plasma membrane targeting. *Cells*. 2019;8:1246.
35. Fallahi-Sichani M, Linderman JJ. Lipid raft-mediated regulation of G-protein coupled receptor signaling by ligands which influence receptor dimerization: a computational study. *PLoS ONE*. 2009;4:8.
36. Sharma M, Celver J, Oceau JC, Kovoov A. Plasma membrane compartmentalization of D2 dopamine receptors. *J Biol Chem*. 2013;288:18.
37. Levental I, Lingwood D, Grzybek M, Coskun Ü, Simons K. Palmitoylation regulates raft affinity for the majority of integral raft proteins. *Proc Natl Acad Sci USA*. 2010;107:51.
38. Bryksin AV, Matsumura I. Overlap extension PCR cloning: A simple and reliable way to create recombinant plasmids. *Biotechniques*. 2010;48:6.
39. Gibson SK, Gilman AG. Gi $\alpha$  and G $\beta\gamma$  subunits both define selectivity of G protein activation by  $\alpha_2$ -adrenergic receptors. *Proc Natl Acad Sci USA*. 2006;103:1.
40. Mystek P, Tworzydło M, Dziedzicka-Wasylewska M, Polit A. New insights into the model of dopamine D1 receptor and G-proteins interactions. *Biochim Biophys Acta (BBA) Mol Cell Res*. 2015;1853:594–603.
41. Lakowicz JR. Principles of fluorescent spectroscopy. 3rd ed. New York: Springer; 2006.
42. Yu JZ, Rasenick MM. Real-time visualization of a fluorescent Gas: Dissociation of the activated G protein from plasma membrane. *Mol Pharmacol*. 2002;61:2.
43. Wood M, Dubois V, Scheller D, Gillard M. Rotigotine is a potent agonist at dopamine D1 receptors as well as at dopamine D2 and D3 receptors. *Br J Pharmacol*. 2015;172:4.
44. Cordeaux Y, Nickolls SA, Flood LA, Graber SG, Strange PG. Agonist regulation of D<sub>2</sub> dopamine receptor/G protein interaction. *J Biol Chem*. 2001;276:31.
45. Scheller D, Ullmer C, Berkels R, Gwarek M, Lübbert H. The in vitro receptor profile of rotigotine: a new agent for the treatment of Parkinson's disease. *Naunyn-Schmiedeberg's Arch Pharmacol*. 2009;379:1.
46. Van der Weide J, De Vries JB, Tepper PG, Horn AS. Pharmacological profiles of three new, potent and selective dopamine receptor agonists: N-0434, N-0437 and N-0734. *Eur J Pharmacol*. 1986;125:2.
47. Adachi N, Yoshimura A, Chiba S, Ogawa S, Kunugi H. Rotigotine, a dopamine receptor agonist, increased BDNF protein levels in the rat cortex and hippocampus. *Neurosci Lett*. 2017;662:51.
48. Horn AS, Tepper P, Van Der Weide J, Watanabe M, Grigoriadis D, Seeman P. Synthesis and radioreceptor binding activity of N-0437, a new, extremely potent and selective D2 dopamine receptor agonist. *Pharm Weekbl Sci Ed*. 1985;7:5.
49. Lane JR, Powney B, Wise A, Rees S, Milligan G. G protein coupling and ligand selectivity of the D2L and D3 dopamine receptors. *J Pharmacol Exp Ther*. 2008;325:1.
50. Senogless SE, Heimert TL, Odife ER, Quasney MW. A region of the third intracellular loop of the short form of the D2 dopamine receptor dictates Gi coupling specificity. *J Biol Chem*. 2004;279:3.
51. Watts VJ, Neve KA. Activation of type II adenylate cyclase by D2 and D4 but not D3 dopamine receptors. *Mol Pharmacol*. 1997;52:2.
52. Bajar BT, Wang ES, Zhang S, Lin MZ, Chu J. A guide to fluorescent protein FRET pairs. *Sensors (Switzerland)*. 2016;16:9.
53. Mystek P, Dutka P, Tworzydło M, Dziedzicka-Wasylewska M, Polit A. The role of cholesterol and sphingolipids in the dopamine D1 receptor and G protein distribution in the plasma membrane. *Biochim Biophys Acta Mol Cell Biol Lipids*. 2016;1861:11.
54. Kusumi A, Fujiwara TK, Tsunoyama TA, Kasai RS, Koichiro AL, Masanao MH, et al. Defining raft domains in the plasma membrane. *Traffic*. 2020;21:106.
55. Gupte TM, Ritt M, Dysthe M, Malik RU, Sivaramkrishnan S. Minute-scale persistence of a GPCR conformation state triggered by non-cognate G protein interactions primes signaling. *Nature Communications*. 2019;10:1.
56. Ungerstedt U. Stereotaxic mapping of the monoamine pathways in the rat brain. *Acta Physiol Scand*. 1971;82:367.

57. Offermanns S, Rosenthal W. *Encyclopedia of molecular pharmacology*. 2nd ed. Berlin: Springer; 2008.
58. Jiang M, Bajpayee NS. Molecular mechanisms of Go signaling. *Neurosignals*. 2009;17:1.
59. Wang Y, Park S, Bajpayee NS, Nagaoka Y, Boulay G, Birnbaumer L, et al. Augmented glucose-induced insulin release in mice lacking Go2, but not Go1 or Gi proteins. *Proc Natl Acad Sci USA*. 2011;108:4.
60. Tang G, Wang Y, Park S, Bajpayee NS, Vi D, Nagaoka Y, et al. G $\alpha$ 2 G protein mediates galanin inhibitory effects on insulin release from pancreatic  $\beta$  cells. *Proc Natl Acad Sci USA*. 2012;109:7.
61. Hilger D, Masureel M, Kobilka BK. Structure and dynamics of GPCR signaling complexes. *Nat Struct Mol Biol*. 2018;25:1.
62. Gacasan SB, Baker DL, Parrill AL. G protein-coupled receptors: the evolution of structural insight. *AIMS Biophysics*. 2017;4:3.
63. Flock T, Ravarani CNJ, Sun D, Venkatakrishnan AJ, Kayikci M, Tate CG, et al. Universal allosteric mechanism for G $\alpha$  activation by GPCRs. *Nature*. 2015;524:7564.
64. Sandhu M, Touma AM, Dysthe M, Sadler F, Sivaramakrishnan S, Vaidehi N. Conformational plasticity of the intracellular cavity of GPCR—G-protein complexes leads to G-protein promiscuity and selectivity. *Proc Natl Acad Sci USA*. 2019;116:24.
65. Semack A, Sandhu M, Malik RU, Vaidehi N, Sivaramakrishnan S. Structural elements in the Gas and G $\beta$ q C termini that mediate selective G Protein-coupled Receptor (GPCR) signaling. *J Biol Chem*. 2016;291:34.
66. Wedegaertner PB. G protein trafficking. *Subcell Biochem*. 2012;63:193–223.
67. Vogler O, Casas J, Capo D, Nagy T, Borchert G, Martorell G, et al. The G $\beta$  dimer drives the interaction of heterotrimeric Gi proteins with nonlamellar membrane structures. *J Biol Chem*. 2004;279:35.
68. Marrari Y, Crouthamel M, Irannejad R, Wedegaertner PB. Assembly and trafficking of heterotrimeric G proteins. *Biochemistry*. 2007;46:26.
69. Kosloff M, Elia N, Selinger Z. Structural homology discloses a bifunctional structural motif at the N-termini of Ga proteins. *Biochemistry*. 2002;41:49.
70. Chen CA, Manning DR. Regulation of G proteins by covalent modification. *Oncogene*. 2001;20:1643.
71. Kleuss C, Krause E. Gas is palmitoylated at the N-terminal glycine Christiane. *The EMBO journal*. 2003;22:4.
72. Borders CL, Broadwater JA, Bekeny PA, Salmon JE, Lee ANNS, Eldridge AM, et al. A structural role for arginine in proteins: multiple hydrogen bonds to backbone carbonyl oxygens. *Protein Sci*. 1994;3:541.
73. Donald JE, Kulp DW, Degrado WF. Salt bridges: geometrically specific, designable interactions. *Proteins*. 2011;79:3.
74. Hristova K, Wimley WC. A look at arginine in membranes. *J Membr Biol*. 2011;23:1.
75. Medkova M, Preininger AM, Yu NJ, Hubbell WL, Hamm HE. Conformational changes in the amino-terminal helix of the G protein  $\alpha$ 1 following dissociation from g $\beta$  subunit and activation. *Biochemistry*. 2002;41:31.
76. Montmayeur JP, Guiramand J, Borrelli E. Preferential coupling between dopamine D2 receptors and G-proteins. *Mol Endocrinol*. 1993;7:2.
77. Žuk J, Bartuzi D, Matosiuk D, Kaczor AA. Preferential coupling of dopamine d2s and d2l receptor isoforms with gi1 and gi2 proteins—in silico study. *Int J Mol Sci*. 2020;21:2.
78. Scarselli M, Annibale P, McCormick PJ, Kolachalam S, Aringhieri S, Radenovic A, et al. Revealing G-protein-coupled receptor oligomerization at the single-molecule level through a nanoscopic lens: methods, dynamics and biological function. *FEBS J*. 2016;283:7.
79. Kasai RS, Ito SV, Awane RM, Fujiwara TK, Kusumi A. The Class-A GPCR dopamine D2 receptor forms transient dimers stabilized by agonists: detection by single-molecule tracking. *Cell Biochem Biophys*. 2018;76:1.
80. Chisari M, Saini DK, Cho JH, Kalyanaraman V, Gautam N. G protein subunit dissociation and translocation regulate cellular response to receptor stimulation. *PLoS ONE*. 2009;4:11.
81. Abankwa D, Vogel H. A FRET map of membrane anchors suggests distinct microdomains of heterotrimeric G proteins. *J Cell Sci*. 2007;120:16.
82. Weinberg ZY, Puthenveedu MA. Regulation of G protein-coupled receptor signaling by plasma membrane organization and endocytosis. *Traffic*. 2019;20:2.
83. Pándy-Szekeres G, Munk C, Tsonkov TM, Mordalski S, Harpsøe K, Hauser AS, et al. GPCRdb in 2018: adding GPCR structure models and ligands. *Nucleic Acids Res*. 2018;46:D1.

## Publisher's Note

Springer Nature remains neutral with regard to jurisdictional claims in published maps and institutional affiliations.

Ready to submit your research? Choose BMC and benefit from:

- fast, convenient online submission
- thorough peer review by experienced researchers in your field
- rapid publication on acceptance
- support for research data, including large and complex data types
- gold Open Access which fosters wider collaboration and increased citations
- maximum visibility for your research: over 100M website views per year

At BMC, research is always in progress.

Learn more [biomedcentral.com/submissions](https://biomedcentral.com/submissions)

